LA-UR-19-29415
Approved for public release; distribution is unlimited.

Title: Micro Reactor Instrumentation and Control FY2019 Report

Author(s): Mascarenas, David Dennis Lee
Meyerhofer, Peter David
Ezell, Dianne
Ramuhalli, Pradeep
Unruh, Troy

Intended for: FY2019 Report

Issued: 2019-09-18

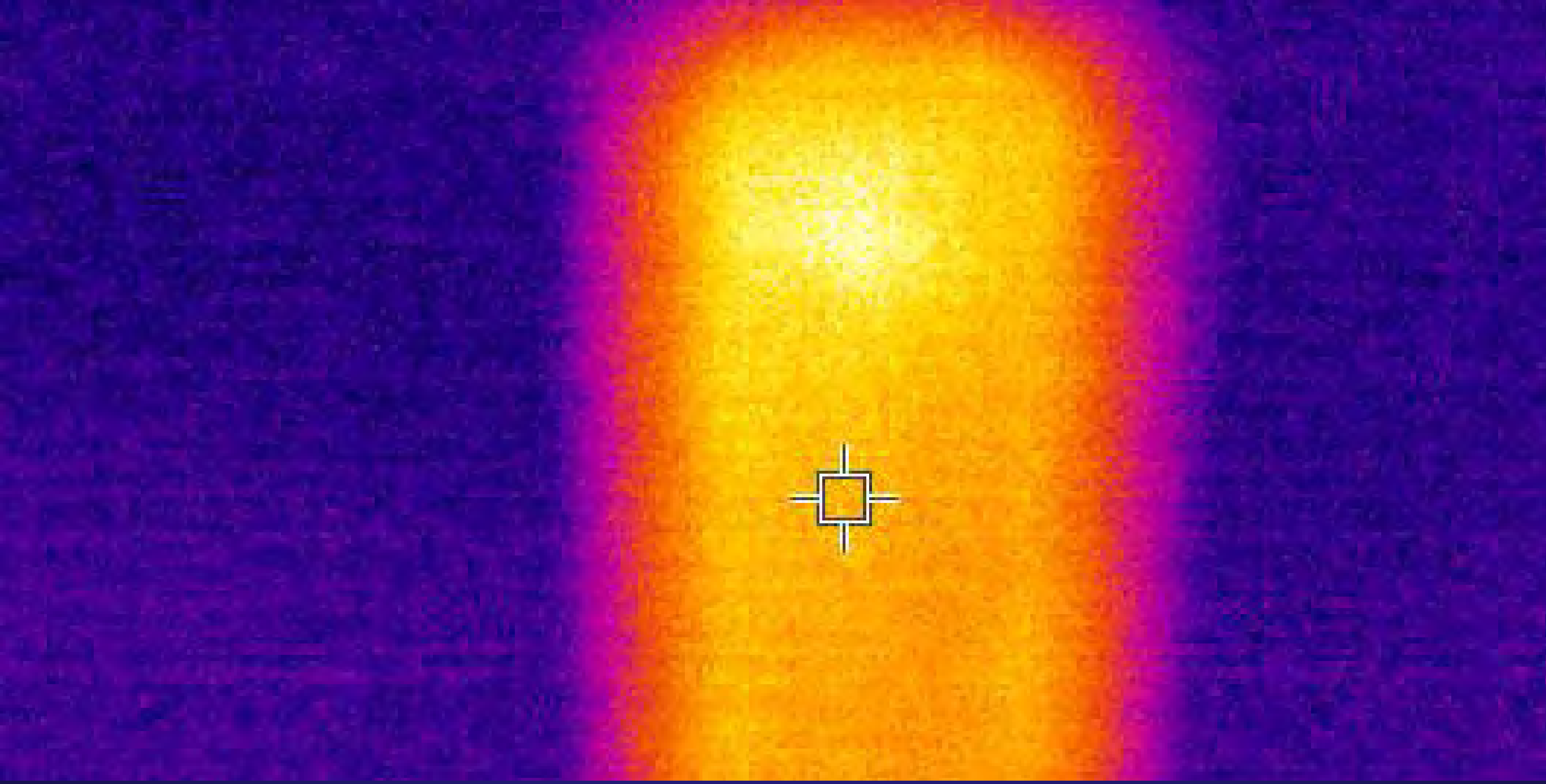

Micro Reactor Instrumentation and Control FY2019 Report

David Mascareñas
Peter Meyerhoffer
Dianne Ezell
Pradeep Ramuhalli
Troy Unruh

9/20/2016

Los Alamos
NATIONAL LABORATORY
EST. 1943

1. Introduction:

Micro-reactors (i.e., very small transportable or mobile nuclear reactors with a capacity less than 20 MWt) are being developed to supply heat and power for various applications in remote areas, military installations, emergency operations, humanitarian missions, and disaster relief zones. A wide variety of reactor types are under consideration, including sodium-cooled fast reactors, molten salt reactors, light water reactors, very-high-temperature gas reactors, and heat pipe reactors. These miniaturized transportable reactor designs remain largely untested and unproven. System and component testing are needed to demonstrate design safety and system robustness, reliability and efficiency.

2. Concept of Operations for Instrumentation for the non-nuclear micro-reactor test bed.

The Department of Energy (DOE) Office of Nuclear Energy's (NE) Micro-Reactor Research, Development, and Deployment (RD&D) Program manages national-laboratory-led early-stage generic research and technology development for micro-reactor systems and provides cost-shared support for micro-reactor vendor development and licensing activities through the DOE-NE Industry Funding Opportunity Announcement. The program also coordinates efforts between the Department of Defense (DoD), industry, and the Nuclear Regulatory Commission (NRC) to support the demonstration of micro-reactor technology on a DOE national laboratory site. National laboratories supporting the Micro-Reactor Program include Idaho National Laboratory (INL), Oak Ridge National Laboratory (ORNL), Los Alamos National Laboratory (LANL), Argonne National Laboratory (ANL), and Sandia National Laboratory (SNL).

A non-nuclear micro-reactor test bed (NMTB) is being developed to assist developing, demonstrating, and validating micro-reactor components and systems. The test bed supports technology maturation to reduce uncertainty and risk relating to operating and deploying micro-reactor systems. Systems and components can be safely tested to failure at the NMTB, giving valuable information regarding failure modes and thresholds. Potential users of the NMTB include micro-reactor developers, energy users, and regulators. Regulators can be engaged early in the design and testing to expedite regulatory approval and licensing.

The test bed will include an enclosure for housing test articles, electrical heaters, cooling system, instruments and sensors, and data acquisition hardware and is configured in a plug-and-play arrangement. Modeling and simulation (M&S) will be employed to design experiments, and the collected data will be used to validate models. This information guides the placement of sensors and helps predict operating performance under a range of normal, off-normal or accident conditions. M&S is also valuable for scaling prototypical hardware for each test. Computational control and model feedback will be pursued to emulate thermal response times and magnitudes of an operating reactor. The overall objective is to test components and systems to verify the safe, reliable and efficient operation of micro-reactor designs.

3. Measurement Needs for micro-reactors

When operational, the testbed is expected to be used for experiments that may require up to 300 hours of continuous testing. The primary intent is to measure quantities that help characterize the elasticity of the test articles and the heat balance during steady state. Consequently, some of the measured quantities that are expected to be of interest are the temperature, pressure, flow rate, power input, power output, and stress state of the test article. These measurements are expected to be required at different locations on and around the test article. For the case of a gas cooled test article (monolith and heat exchanger), specific quantities of interest include [1]:

1. Electrical power to evaporator
2. Volumetric flow rate of gas at heat exchanger entrance
3. Pressure of gas at heat exchanger entrance
4. Evaporator entrance temperature
5. Evaporator midpoint temperature
6. Evaporator exit temperature
7. Condenser entrance temperature
8. Condenser midpoint temperature
9. Condenser exit temperature
10. Core strain (reactivity feedback, elastic deformation, creep)
11. Heat exchanger strain reactivity (elastic deformation, creep)
12. Core stress state
13. Heat exchanger stress state
14. Heat exchanger guard heater power (as applicable)
15. Thermal gradient across core insulation (as applicable)
16. Thermal gradient across heat exchanger insulation (as applicable)

In addition to the process and structural integrity parameters above, deployed micro-reactors are also expected to require measurements of the neutron and gamma fluxes. Additional measurement needs may arise with specific micro-reactor designs and will be addressed on a case-by-case basis in future reports.

4. Prior Instrumentation Work Relevant to Monitoring the non-nuclear micro-reactor test bed.

Inspecting nuclear power plants is especially important due to the risk of leaking radioactive material. Rao [2] describes how the thickness of feeder pipe elbows is evaluated ultrasonically, though this does not access the structure of the core. In 2011, Rempe et al evaluated several candidate technologies for taking measurements in nuclear reactors [3]. Fiber optics are useful for noncontact distributed measurements, but darken over time when exposed to radiation, while electrical conductivity sensors can detect cracking and porosity in the fuel rods by corresponding changes in the conduction path. Ultrasonic sensors require surface contact but are suited for measuring temperatures above 2000 °C through changes in the speed of sound [4]. Sun et al [5] developed a multimode sensor for a dry storage cask that uses acoustic emission to detect the onset of damage, then an ultrasonic method to locate the damage. Lin et al [6] considered the use of a thermoelectric generator to power sensors on a reactor. Holbert et al [7] tested various commercial sensors for resistance to pulsed radiation. Accelerometers can be used to detect vibration or looseness in parts such as pipe connections [8]. Moisture sensors (to detect steam leaks) and strain gages have also been reported [9].

The report [8] consider the viability of a range of sensor technologies for recent reactor designs. Optical sensing has the potential to detect temperature and pressure changes at distributed locations with a relatively safe standoff, though one must choose materials carefully for strength, reactivity, temperature resistance and radiation resistance. The temperature range of many fibers is limited by the coatings and claddings deposited onto them to improve mechanical properties. Several optical materials, such as diamond for windows and molybdenum for mirrors, are promising for optical components. Radiation-hardened cameras require some testing but are well-developed; thermal cameras largely have not been tested for radiation resistance. Pyrometers, which measure temperature by the intensity of grey-body emission at different wavelengths, are known to work near 3000 °C even with a combined surface and lamp [10]. Sensors based on semiconductor bandgaps, which vary with temperature and are insensitive to some physical disturbances, are largely unsatisfactory for temperature and radiation exposure. Backscattering time-domain reflection can locate disturbances within a meter on a kilometer-long fiber based on the return of a laser pulse, but has not been tested for radiation resistance (for use near the core). The same is true of Fabry-Pérot temperature sensors, based on a pair of reflective surfaces in a fiber to create an interference cavity, which might also serve as pressure sensors if one end of the cavity is a flexible membrane. Such temperature-dependent properties as birefringence and fluorescence lifetime are unlikely to be feasible in practical sensors. Laser Doppler vibrometry is a candidate for deflection measurements, if the coolant is transparent and the sensor can be isolated from base vibrations.

A conventional temperature measurement [9] uses thermocouples up to 1300 °C (or resistance temperature detectors [11]) and strain gages to monitor reactor conditions. Another temperature sensing method is Johnson noise, based on the statistical fluctuations of electrical fields which depends solely on absolute temperature. However, that signal is faint and difficult to calibrate reliably. The most popular pressure sensing method is an impulse line that removes the electronics to less harsh environment. Fabry-Pérot sensors can operate up to 1200 °C [12].

Fiber Bragg gratings have received much attention in recent years for radiation applications. These periodic modulations of refraction index in an optical fiber have a reflection peak that changes wavelength with temperature, allowing temperature measurements. However, radiation exposure causes a separate change in reflection wavelength due to imperfections, obscuring those measurements [13]. More recent work has considered how to reduce the error in such temperature readings up to 350 °C [14] [15]. Optical fiber techniques have also been applied to interferometry for displacement measurement [16], and extended with silica to 1000 °C [17] at which radiation-induced darkening tends to decrease [18]. Single-crystal sapphire fibers are highly radiation resistant [19] and have been demonstrated in Bragg gratings up to 1700 °C [20]. Such gratings can also measure pressure above 800 °C [21].

Figure 1 shows several of the measurements cited above, with the associated temperatures and objectives.

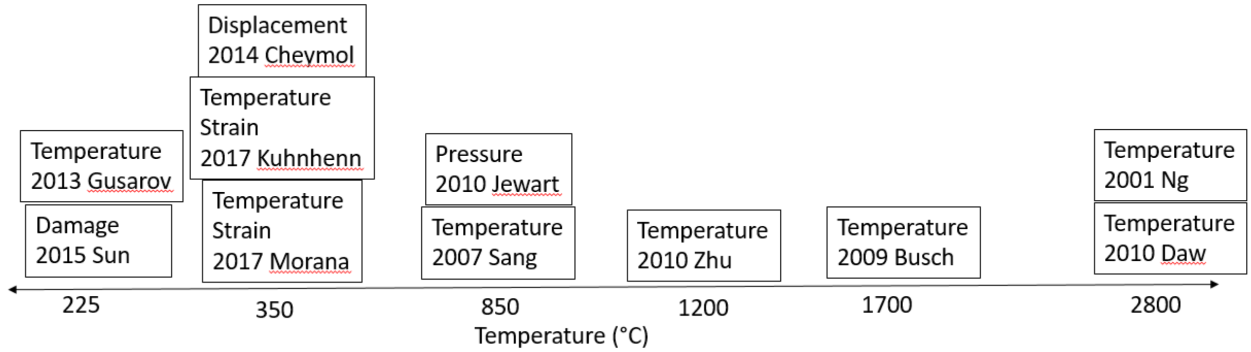

Figure 1: Temperatures and measurement objectives of past works cited in this section.

Heat pipes have been built and tested up to the temperature range of liquid metals, primarily using thermocouples to monitor temperature. The temperatures concerned were 600 °C for a space station test [22] and 1000 °C for a ceramic heat pipe test [23] (the latter also used a thermal camera). On a smaller scale, thin film thermistors and pressure transducers have been used on micro heat pipes meant for electronic circuits below 100 °C [24] [25].

In-Pile Instrumentation Program

The capability to monitor the conditions inside and near nuclear reactors is considered essential to aid in the development of reactor designs including proposed micro-reactor designs. In response to the need for condition monitoring of reactor components the Department of Energy has added an additional element to the Nuclear Energy Enabling Technologies (NEET) Advanced Sensors and Instrumentation (ASI) program known as the In-pile Instrumentation (I2) program [26]. The I2 program serves to discover, demonstrate and secure innovative nuclear energy solutions through the research, design, development and deployment of nuclear instrumentation. Sensor technologies are systematically matured from a low technology readiness level (TRL) to a higher TRL in the program to aid the researchers, developers and vendors in the nuclear energy community.

The I2 crosscutting technology development program is researching several sensors that may be of interest to micro-reactors programs using the NMTB that is currently under development. These sensors are summarized by the measurement of interest below.

a. **Thermal measurements:** Temperature detection sensors under investigation as part of the I2 program that may be of interest to users of the NMTB include the High Temperature Irradiation Resistant Thermocouple (HTIR-TC), optical fiber based temperature sensors, and the ultrasonic thermometer (UT).

   HTIR-TC: HTIR TCs are sheathed thermocouples based on molybdenum and niobium alloys as sensing element. There thermocouples resist degradation from transmutation during irradiations that are typically encountered in commercial thermocouples using in irradiation environments.

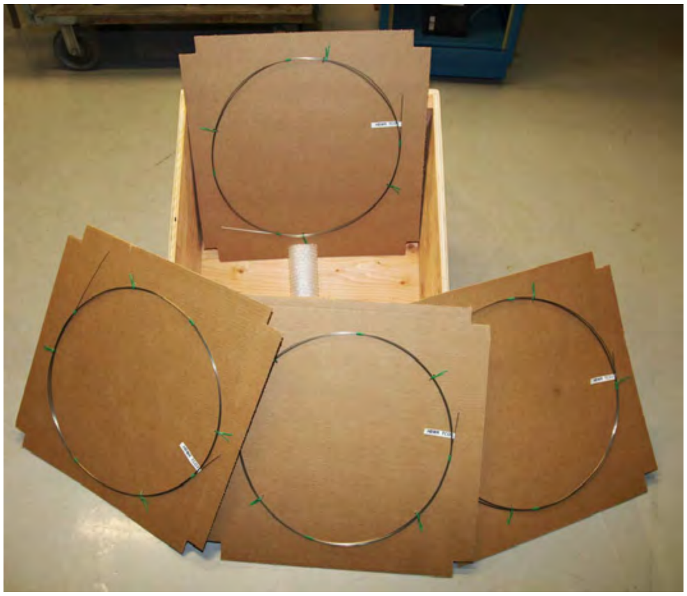

Figure 2: HTIR-TCs for irradiation testing.

Activities in I2 have focused on selection of sheath material composition; insulation material; and refinement of the heat treatment process [27]. In addition, HTIR-TC as shown in Figure *2* have been commercialized as part of the DOE's Technology Commercialization Fund (TCF) to be considered for widespread use in all high temperature nuclear reactor applications up to 1600 °C. A comparison of the HTIR-TC against other thermocouples is outlined in Table 1 below:

Table 1. Comparison of commercially available thermocouples with the HTIR-TC:

Thermocouple	Type K	Type B	Type N	HTIR-TC
Materials	Chromel vs Alumel	PtRh30% vs PtRh6%	Nicrosil vs. Nisil	Molybdenum vs. Niobium
Temperature Range	-270°C to 1260°C	250°C to 1700°C	-270°C to 1260°C	0°C to 1700°C
Cost	~$30/ft	~$250/ft	~$50/ft	~$250/ft
Radiation Tolerance as Compared to HTIR-TC	1/10th	~1/100th	1/4th	

This thermocouple may be of interest to micro-reactor researchers because it can deployed similarly to commercial thermocouples, but offers an extra level of irradiation resilience.

Optical fiber based temperature sensors: Thermal measurements based on optical fibers offer small intrusion, intrinsic immunity to electromagnetic interference, and wide availability at a reasonable cost. The use of optical fiber based temperature measurements is already being leveraged in Transient Reactor Test (TREAT) Facility experiments through infrared pyrometry. Additional research includes Fiber Bragg Gratings (FBG) in the Advanced Test Reactor (ATR) [28] as shown in Figure 3 and distributed optical sensing techniques.

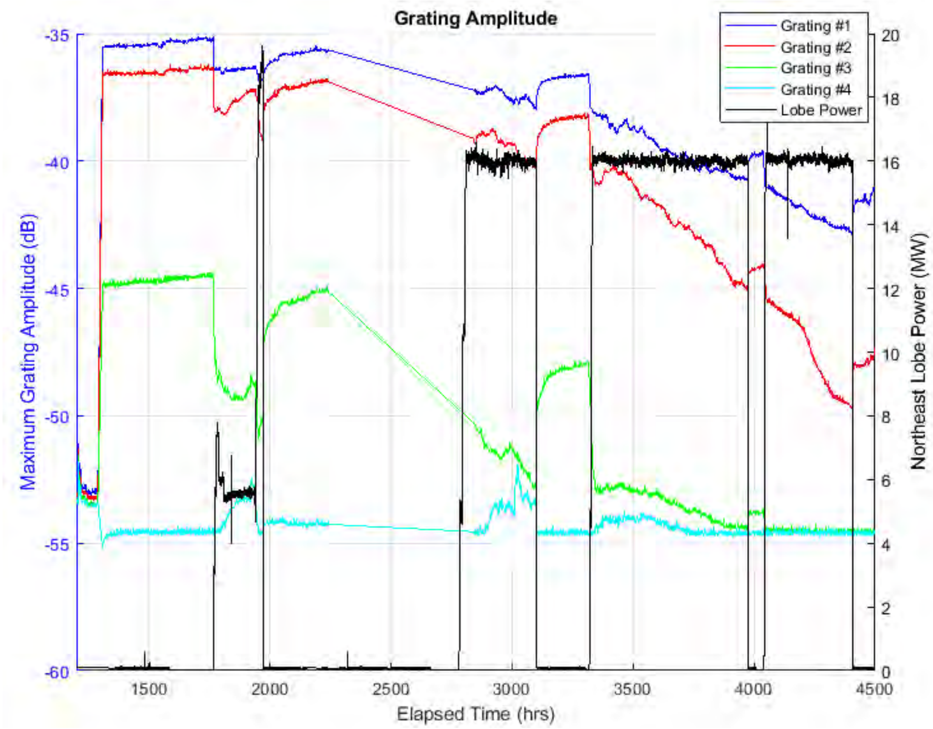

Figure 3 Optical fiber grating amplitude in ATR irradiation

Most recent irradiation activities focus on FBG sensors due to their maturity in other industries and stability in high temperatures. Optical fiber temperature sensors may be of interest to micro-reactor researchers because of the small size and immunity to electromagnetic interference.

Ultrasonic Thermometer: UTs utilize a single small diameter probe to obtain distributed temperature measurements using a multi-segment sensor. UT based temperature measurements may be made near the melting point of the sensor material which offers the potential to measure temperature in excess of 3000 °C. With proper design, UTs may use structural materials as wave guides to infer temperature measurements. UTs have recently demonstrated distributed temperature measurements in the ATR [29] with improved radiation resilience as shown in Figure 4.

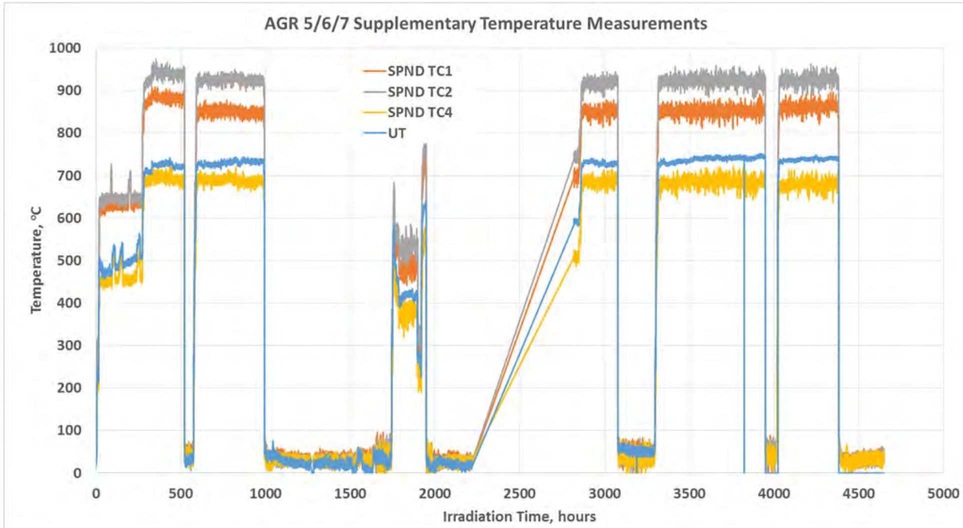

Figure 4 UT signal in ATR irradiation test

UT sensors may be of interest to micro-reactor researchers because of the ability to directly interrogate components for temperature measurements.

b. **Dimensional measurements:** Dimensional sensors for reactor measurements are typically performed with a Linear Variable Differential Transformer (LVDT) due to the excellent performance under irradiation conditions. LVDTs for irradiation testing have been developed by the Halden Reactor Project (HRP) for a number of different dimensional measurements including cladding and fuel elongation measurements. The recent closure of HRP has prompt the I2 program [26] to facilitate technology and knowledge transfer for LVDT technologies to ensure availability for these specialized measurements. LVDTs may be of interest to micro-reactor researchers needing dimensional measurements because of the performance record in irradiation testing conditions.

c. **Pressure measurements:** Pressure sensors for in-reactor measurements are typically performed with LVDTs by coupling with a bellows as was routinely performed at the HRP and is being researched as part of I2 [26]. Optical fiber-based Fabry-Perot pressure measurements are also being explored as a part of I2 fiber optic activities starting in FY20. The pressure sensors may be of interest to micro-reactor researchers needing radiation resilient pressure measurements in the case of LVDTs or small intrusion measurements in the case of fiber-based measurements.

d. **Nuclear measurements:** Nuclear sensors are not necessary for the NMTB, but are mentioned because of the eventual need for testing in a nuclear fueled micro-reactor testbed. The Self-Powered Neutron Detector (SPND) and fission chamber are sensors commonly used for measurement of neutron flux in nuclear reactors. A new vendor for specialized self-powered neutron detectors has been identified as part of I2 to meet the needs of TREAT irradiations [30].

5. Overview of Sensing Modalities to Evaluate for Monitoring the Integrity of the Monolithic Structure

Monitoring the monolith, heat pipes, and containment is important to ensure reliable reactor performance. Traditional instrumentation relies on instrumentation ports and feedthroughs to access points of interest on the reactor. However, there is still a level of isolation between the sensor and reactor. Embedded sensors allow for a more coupled measurement. Oak Ridge National Laboratory (ORNL) has been developing techniques to embed sensors enabling on-line structural health monitoring, in-situ weld inspections, and distributed sensing. Some of the sensors of interest are temperature, pressure, flow, strain/deformation, heat flux, damage/plastic deformation. We now summarize some of the applicable technologies.

a. **Ultrasonic Phased Arrays:** Ultrasonic phased array systems offer a convenient method for detecting the presence of defects in structures and may offer a method for monitoring the monolith in a NMTB. When using such systems, the monolithic structure will need to be instrumented with an array of piezoelectric sensor/actuators. We would excite the structure using a subset of the piezoelectric patches and then record the response using another subset of piezoelectric patches. We would then apply statistical classification techniques to the response measurements to try and infer the presence of damage in the structure. A key challenge in applying this technique in the NMTB is the high temperature environment that the piezoelectric array will encounter. High-temperature (500-800 °C) tolerant piezoelectric materials have been explored in the past for use under such conditions [31] (including the possibility of phased array transducers), and will need to be adapted to this application. Note that ultrasonic techniques (including the use of ultrasonic phased arrays) can be used for direct measurement of dimensional changes in structures [32] and fuel [33], [34] and may provide a measure of the strain in the structure.

b. **Acoustic Emission Sensors:** If the joints in the monolithic structure crack or are otherwise damaged, they will almost certainly emit an acoustic signal. We would like to instrument the monolithic structure with an array of acoustic emission sensors. We would then use the data from this array of acoustic emission sensors to try and detect and localize the presence of damage in the monolithic structure. In a similar manner to ultrasonic phased array systems, high-temperature tolerant sensors will be needed. Again, high-temperature piezoelectric materials may be used directly for acoustic emission monitoring. An alternative arrangement using AE sensors on waveguides is also a possibility [35] and allows the transducers to stand-off from the structure being monitored.

c. **Laser Doppler Vibrometer with Steering Mirror:** A laser doppler vibrometer could possibly be used to achieve many of the same goals as the acoustic emission sensors. The difference would be that the laser Doppler vibrometer acts in a stand-off manner. The ability to capture structural vibrations remotely could be important for the monolithic structure when it is operating at high temperatures that could damage traditional sensors.

d. **Interferometry coupled with Full-field, High Resolution Video-Based Structural Dynamics:** The LANL Engineering Institute (LANL-EI) has developed an algorithm to automatically extract full-field, high resolution mode shapes of vibrating structures from video. This approach is unique among video-based structural dynamics techniques because it does not require the use of any marker or speckle pattern on a structure of interest. It is highly likely that this class of techniques could be applied to data captured using a laser interferometer. We think it would be fruitful to combine these measurements with seismic imaging analysis to attempt to "see" inside of the monolithic structure.

e. **Accelerometers:** We would like to instrument the monolithic structure with an array of accelerometers that could be used to measure the resonant frequencies, mode shapes and damping ratios of the monolithic structure. We would then study changes in the structural response that could be indicative of damage. We would also use our video-dynamics algorithms in conjunction with the accelerometer data to try to effectively increase the resolution of our mode shape measurements.

f. **Thermal Imagers:** Many different forms of damage result in the emission of a thermal signature. For example damage in a structure could lead to unintended rubbing of components, or loss of thermal conductivity which often lead to hot spots in a structure that can be detected using thermal imagery. It is anticipated that damage in the monolithic structure's joints will lead to changes in the thermal behavior of the monolithic structure which could be used to infer the presence of damage in the structure.

g. **Ultrasonic Guided Waves**: Ultrasonic guided waves provide another option for monitoring the monolith and detecting the presence of damage in the structure. Essentially, guided waves are stress waves that are guided by the structure boundaries; interactions with an inhomogeneity in the structure result in a change in the received signal that can be interpreted through the use of finite element models. Simulation studies indicated the potential for high sensitivity of such measurements in structures that are adjacent to liquid Na [36]. However, the interpretation can be challenged by the presence of complex structures and multiple geometric changes/material changes. Again, there is a need for high-temperature enabled ultrasonic sensors (piezoelectric or magnetostrictive) for use in the NMTB. If applied to monitoring components in a micro-reactor, additional requirements on survivability in a radiation environment will need to be applied to the sensor.

h. **Resonance Inspection**: This is another technique in a line of ultrasonic-based methods that have been proposed for structural monitoring and defect detection[1]. The technique may be applied to detect the presence of a defect (but not necessarily its location) in a structure based on changes in its natural frequency spectra. While some advances have been made towards quantifying the defect characteristics [37], the technique is still likely to be useful as a method for screening tool to identify the presence of a defect that other techniques may be used to characterize (location, severity) after the detection step.

i. **Strain Gauges/Stand-off Displacement Sensors**: It is anticipated that damage in the monolithic structure will result in deformations of the structure. We would like to track these deformations using arrays of strain gauges and Stand-off displacement sensors. The measurements from these sensors could be combined with analysis from finite element models to try and infer damage inside of the structure.

j. **Optical fiber strain sensors:** The instrumentation needs between the test article that will be testing in the NMTB and the final reactor design are somewhat different. For example, sensor placement will be slightly different due to sensor density or availability to make contact with the test article, cabling feedthroughs and temperature gradient across the cables, temperature gradient across the reactor, assembly of the experiment into and out of the test bed, and data acquisition parameters. This document elaborates on the embedding of sensors in more detail. One conceptual design to monitor thermal stresses in a heat pipe is shown in Figure 5.

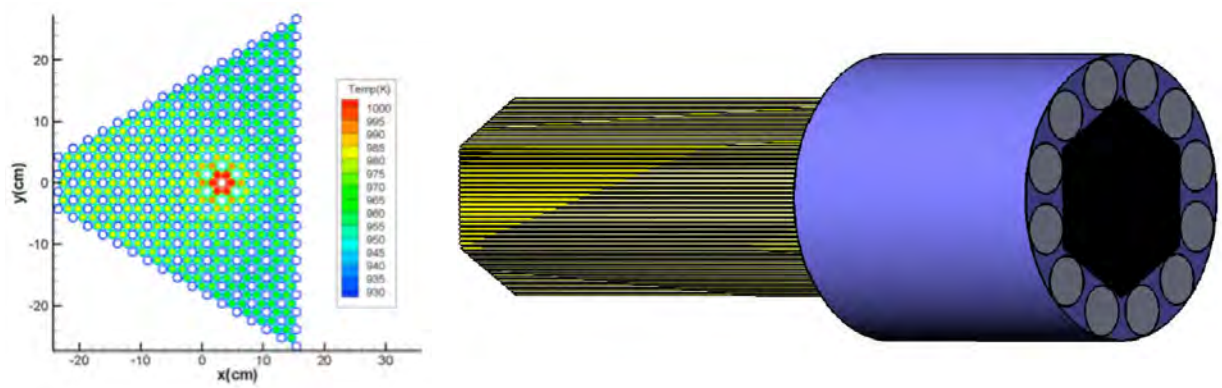

Figure 5 Potential monitoring of thermal stresses in monolithic heat pipe-based micro-reactors *[38]*

Material selection will be critical for the embedded sensors because of the structural durability of the sensor, easing the embedding processing, and survivability in the irradiation field. For stress monitoring, the fiber requires direct coupling with the materials [28]. Therefore, a standard fiber insulator is not sufficient and requires a metallic coating or sheath. One technique developed at ORNL to embed fiber optics into metals applied ultrasonic additive manufacturing, see Figure 6. Multiple coatings were tests and demonstrated successful embeddings at temperatures greater than 500°C, see Figure 7. The strain matched expected thermal strain, indicating fibers were well bonded to the surrounding metal structure.

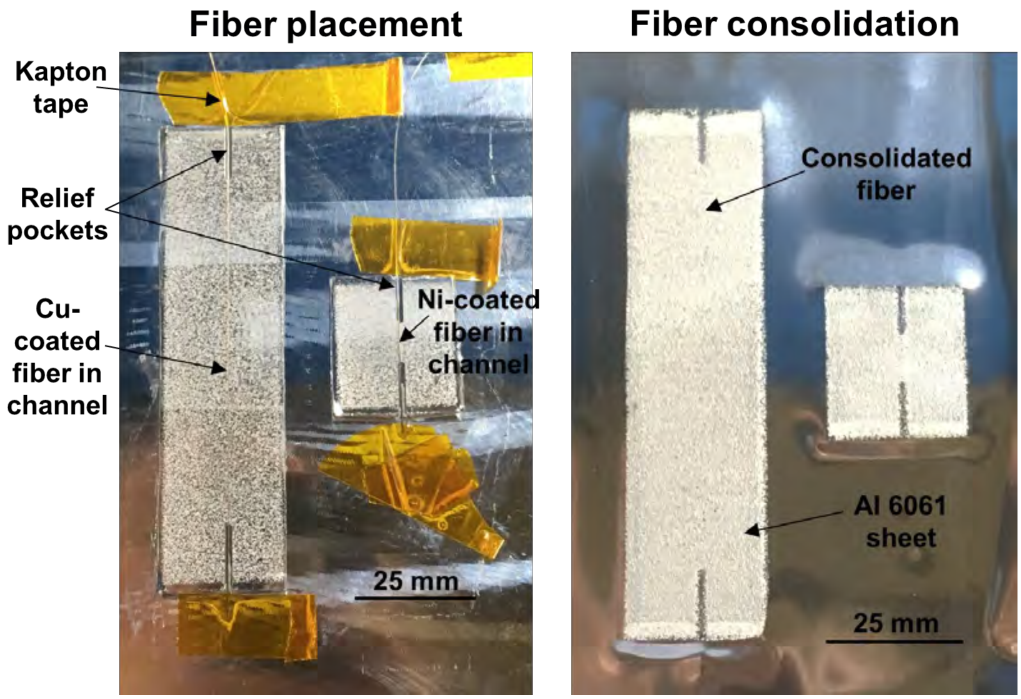

Figure 6 Fiber optic sensor embedding process [2]

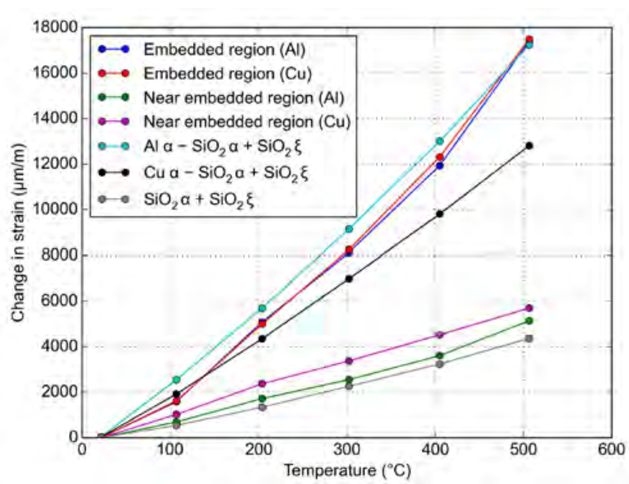

Figure 7 Strain vs. temperature for fibers embedded in Al [3]

It is possible to apply this technique to both the monolith and the heat pipes. The data acquired from these measurements could then be applied for better structural health monitoring during start-up and full power operation of the reactor. Also, applying other embedding techniques would allow for distributed monitoring of temperature, flow, and pressure.

6. Visual Based Techniques for Instrumentation

Visual imaging methods that may be used to monitor the behavior of the monolith, manufacturing process or other components in the NMTB. Optical fiber-based methods are not included in this section though fiber-based methods may provide one approach to visual examination. Imaging techniques to be explored may include:

a. Digital Image Correlation (DIC)

DIC is a technique for finding two-dimensional displacements of a surface that can be extended to three dimensions with an application of camera geometry [39]. For a two-dimensional position vector $\boldsymbol{x}$, let $F(\boldsymbol{x})$ be the gray value intensity of the reference image and $G(\boldsymbol{x})$, of the deformed image. Integer values of the components of $\boldsymbol{x}$ can be taken as corresponding to exact pixel locations, with subpixel intensities found by interpolation. The goal of digital image correlation is to find the displacement $\boldsymbol{d}$ that minimizes

$$\chi^2(\boldsymbol{d}) = \sum (G(\boldsymbol{x}+\boldsymbol{d}) - F(\boldsymbol{x}))^2$$

Equation 1

Where the sum is taken over a subset (often a square grid) of positions $\boldsymbol{x}$ near the point of interest. The iteration step is from $\boldsymbol{x}$ to $\boldsymbol{x}+\boldsymbol{\Delta}$ in the argument of F (the inverse method [40]). Then a first-order minimum with respect to $\boldsymbol{\Delta}$ can be calculated at the position

$$H\boldsymbol{\Delta} = \boldsymbol{b}, H = \begin{bmatrix} \sum\left(\frac{dF}{dx}\right)^2 & \sum\frac{dF}{dx}\frac{dF}{dy} \\ sym & \sum\left(\frac{dF}{dy}\right)^2 \end{bmatrix}, \boldsymbol{b} = \begin{bmatrix} \sum\frac{dF}{dx}(G-F) \\ \sum\frac{dF}{dy}(G-F) \end{bmatrix}$$

Equation 2

Finally, the estimated displacement $\boldsymbol{d}$ is updated to $\boldsymbol{d}-\boldsymbol{\Delta}$ until $\boldsymbol{\Delta}$ is smaller than the chosen tolerance. Another variation on DIC, more suitable for large displacements, combines pure translation with rotation and shear for the affine set of transformations [39].

DIC can also be extended to three dimensions. This requires, as the first step, calibrating two cameras against a target with features of known size and distance, to determine the cameras' relative positions in space as well as their internal parameters [39]. Then the subset in camera 1 is correlated with the same pattern in camera 2 and each respective image location is used to construct a line in three-space through the origin of the camera frame and the given center point in the image plane. The pair of lines established in this way should intersect, but probably do not because of small errors. Still, their closest approach estimates the three-dimensional location of the given subset [41].

The two cameras can take another pair of pictures after deformation. Estimating the three-dimensional position of each subset in the reference frame of camera 1 both before and after (correlating the camera 1 reference subset with both deformed images) gives the calculated three-dimensional displacement.

The whole correlation process depends on having a high-contrast, irregular speckle pattern in which individual speckles are 3-5 pixels wide [39]. This is an additional challenge above 800 °C because many speckle materials will melt, warp and/or have low contrast against the red glow of the substrate. High-temperature speckles can be formed, however, from ceramic oxides mixed with liquid adhesives [42], heat-resistant paints [43] or a roughness pattern scratched on the surface with silicon carbide paper

[44]; one author reached 2600 °C by using several filters and spraying tungsten particles on carbon fiber [45]. All the investigators in the previous sentence eliminated the red background glow with a blue band pass filter in front of the camera.

b. High-resolution, Full Field Techniques

DIC is one way of providing high-resolution displacement and strain data across a whole surface. Another tool for birefringent materials such as plastics under stress, or to filter out surface glare, is polarization. In a recently developed camera [46], each pixel is divided into four at 0°, 45°, 90° and 135° polarization. On the opposite end of the field-of-view spectrum, one team developed a self-calibrating fiber-optic endoscope the size of a few human hairs that can see structures inside a cell [47]. Small vibrations in the image target cause Doppler shifts in the wavelength reflected back to the source, a fact which has been exploited to extract salient frequencies in the terahertz band [48]. Several variations on phase retrieval algorithms have been developed, derived originally from x-ray diffraction [49].

Assembling a grid of cameras with overlapping fields of view can both overcome the tradeoff between resolution and object size, and provide for three-dimensional stereo-matching [50]. High-resolution features that are compromised by increasing the depth of field can be reconstructed computationally [51], for example by applying a speckle pattern [52]. Fusing data from single-photon cameras and CCDs can build on the time resolution of the former and the high pixel count of the latter [53]. Single-photon cameras are also capable of distinguishing depth layers many km from the object [54] [55].

Ghost imaging is a recent method in which the reference beam lands on a conventional (multi-pixel) camera while the other split of the beam is scanned across the image plane before landing on a bucket (single-pixel) detector. The spatial correlation between the two signals then gives an image of the absorption across the sample, as demonstrated with a stream of entangled photons [56] and with incoherent light (in an imaging or a diffraction arrangement) [57]. In computational ghost imaging, there is only the bucket detector and the reference pattern is calculated from a known modulation [58] [59].

Interferometry has been used at high temperatures, and when performed properly is known to be accurate at 800 °C [60]. In one test, it was limited by the decomposition of a platinum-film mirror inside the furnace, at 725 °C [61]. Electronic speckle pattern interferometry has been shown up to material temperature limits (1500 °C for an iron-chromium-aluminum alloy): either surface reactions that obscure the fringes, or the turbulence of melting. The solid skin of a partly molten surface does, however, display high-contrast fringes [62]. A similar method has been used as photogrammetry to compare two pictures of speckle halos up to 870 °C [63] and in the comparison of two holograms of a vibrating plate up to 1000 °C [64].

Moiré interferometry is a technique based on the tendency of two diffraction gratings to produce a coarser set of bright and dark bands. One of the gratings is virtual, caused by the interference of two mutually coherent light beams at a small angle to each other [65]. The key to performing such a measurement at high temperatures is to optimize the physical grating on the sample. By etching the grating into a thin coating of metal, temperatures above 1000 °C are survivable [66] [67]; one author achieved 1370 °C by using a ceramic refractory paint to bond a nickel mesh grating on the specimen [68]. Applications include the study of creep crack growth in metals at 650 °C [69].

Compressive sensing is a method that uses far fewer samples to reconstruct a signal or image than would normally be required by the Nyquist limit of twice the maximum frequency. It accomplishes this by exploiting sparsity, where the signal has few large coefficients in some transform domain, and by minimizing an alternative to the Euclidean norm that promotes sparsity [70] [71]. The idea could be applied to compensate for data lost in wireless transmission [72], or reduce the number of required sensors for event classification in a system [73]. There have also been applications to the low spatial resolution of fiber endoscopes [74], the development of low-cost infrared cameras since high resolution in that range is expensive [75], reducing the readout requirements of imaging in visible and infrared [76] and the encryption of audio signals [77]. The measurement matrix involved in the algorithm can be produced in a variety of ways [78].

c. Non-Line of Sight Imaging

A pulsed laser can be used to track reflection paths around a wall and thereby reconstruct the front contours of a surface [79] [80] [81]; however, the intensity of returned light fades quickly with increasing distance, so one needs a single-photon detector and a long recording time. (For a review, see [82, pp. 13-15].) The same can be done more easily using sound [83] or using infrared wavelengths to detect a hot object [84]. Some variations use spatial coherence [85], a time-of-flight camera [86], a streak camera [87], intensity difference optimization [88] and digital holography [89]. The use of virtual wave fields can imitate line-of-sight imaging and account for multiple reflections [90]. Algorithms also exist for determining a convex room shape by listening to echoes [91]. A simplified version has been demonstrated with differential scattering [92].

Stochastic methods can be used to reconstruct the signal from all photons through a thick scattering medium, as opposed to just the minority of photons with a special property [93]. Others have used a single-photon multi-pixel camera with an optimization solver [94]. There has also been work on lensless cameras that correlate the image through a diffuser plate with the image of a point light source [95]; the idea has also been extended to 3 dimensions [96] and to viewing both forward and backward [97]. The speckles that pass through the scatterer can be interpreted by autocorrelation [98] or a folded-wave interferomoter [99]. Variations include extracting color from a monochrome exposure [100].

Seismic imaging sends acoustic waves into the ground and interprets the return signals to deduce the location and intensity of reflectors [101]. The other objective is to refine a model of the speed of sound throughout the underground volume, which can be done by computationally expensive methods such as tomography and comparison to experimental data [102].

A class of solution methods inspired by quantum physics (scattering in the Schrodinger equation) use integral equations such as those of Gelfand-Levitan and Marchenko to deduce reflection coefficients, and are best-developed in one dimension [103] [104]. One way of accomplishing this is to reconstruct the Green's function (the impulse response at the surface to a virtual source inside the medium, down-going or up-going) [105], which can be extended to multiple spatial dimensions [106]. Recent work has focused on removing the artefacts from multiple reflections [107] [108].

Thermography is another category of inspection methods, where a transient heat source is applied to the structure and temperature deviations on the surface correspond to structural deviations in the material [109]. Pyrometers can use the emitted intensities at two different wavelengths to estimate the temperature in that process up to 1200 °C [110] [111]. Such methods are limited to wide defects very near the surface (such as adhesive failure in laminated sheets) due to the diffusion of heat in three dimensions. Aerospace, in particular, applies such techniques to the inspection of laminated composites [112]. Vibrothermography excites the piece with ultrasonic vibrations (as opposed to heating lamps) so that cracks and other flaws heat up, while recording the surface temperature. The heat from a subsurface flaw propagates to the surface, and the time history of surface temperature can be fitted to the depth of the flaw [113]. Theoretical models of the heat emanating from different kinds of flaws (in points, lines or planes) provide further information. In a different line of inquiry that so far remains computational, surface temperature measurements can also be used to estimate the size and positon of cavities inside a heat conductor [114] [115].

Since waves are time-reversible (wave equations have only second-order time derivatives), playing them backwards allows refocusing at their source even after they have radiated out. This process does a good job of refocusing a sound pulse [116] [117]. Counterintuitively, a greater number of reflection paths actually focuses the reemitted signal more tightly because the effective aperture is larger, reducing diffraction effects [118]. The same has been done with water waves by using a reverberating tank [119]. For electromagnetic waves, time reversal is possible with radio waves [120] and with infrared carried by fiber optic cables [121].

Please note that the measurement data from some of these sensors may eventually act as input to autonomous control and operation technology for micro-reactors. Among the types of information that will be necessary for autonomous control include the process parameters (temperature, pressure, flow rates, and in the case of an operational micro-reactor, neutron and gamma flux) and structural integrity information. The expectation is that such information will be applied to assess the current condition and assess the likely impact of changes to the condition before control action is taken[2].

7. Proposed Instrumentation Efforts for FY2020

a. Los Alamos National Laboratory

Development of capabilities for monitoring micro-reactor health of heat pipe and gas-cooled micro-reactors

- Identify micro-reactor characteristics to be monitored (e.g. strain, temperature, fluence)
- Identify and develop technologies for micro-reactor component health monitoring (coordinate with NEET ASI)
- Develop plan for structural testing monitoring in non-nuclear micro-reactor test-bed.
- Help support identification of sensor and instrumentation needs and operational concepts for autonomous and remote operation and non-nuclear test bed operation.

b. Idaho National Laboratory:

Development of instrumentation/sensor needs to support nonnuclear test bed

- Develop plan for demonstration testing in non-nuclear test bed for micro-reactor systems
- Help identify micro-reactor characteristics such as component health monitoring to be measured (e.g. strain, temperature, fluence)
- Develop and deploy I&C technologies for non-nuclear test bed operation
- Support near-term sensor in-pile testing plan

c. Oak Ridge National Laboratory

ORNL is uniquely aligned to support the micro-reactor instrumentation and control development through the following items:

1. Embedding fiber optic sensors in stainless steel to support testbed monitoring
    a. Evaluating embedded metal-coated fibers at relevant temperatures
    b. Evaluating embedded metal-coated fibers with relevant temperature gradients
2. Evaluating the potential for fabricating Bragg grating sensors (more tolerant to radiation) with metal coatings for eventual implementation in a nuclear test
    a. ORNL is looking into electroless metal deposition and electroplating
3. Developing high-temperature fiber optic feedthroughs using additive techniques
    a. ORNL is evaluating one design with a commercial partner (Luna) that would be interested in marketing this as a product for commercial distribution.
4. Potentially consider embedding other sensors such as thermocouples
5. Providing other support for spatially distributed fiber optic temperature sensing
6. Development of control logic
    a. Autonomous control enables the ability for a central control room to monitor multiple reactors in parallel.
    b. ORNL has a test bed available for testing control logic software that can be slightly modified for multiple control schemes
7. Radiation-tolerant electronics development
8. Low-cost, disposable, printed sensors

Conclusions:

In FY2019 the micro-reactor instrumentation team has spent significant effort surveying the state-of-the-art in sensors and diagnostics for structural monitoring. The team has identified a number of both non-contact, as well as contact sensing approaches that could be applicable to monitoring the manufacture and operation of the reactor monolith as well as associated hardware. Based on this survey, and meetings organized by the cross-lab instrumentation team, a path forward to perform an evaluation of the instrumentation needed to assess the structural integrity of the micro-reactor and its associated manufacturing processes in FY2020.

References:

[1] "National Laboratory Nonnuclear Micro reactor Testing Objectives and Requirements," 2019.

[2] G. Rao, "In-Service Inspection and Structural Health Monitoring for Safe and Reliable Operation of NPPs," *Procedia Engineering,* vol. 86, pp. 476-485, 2014.

[3] J. Rempe and e. al, "New In-Pile Instrumentation to Support Fuel Cycle Research and Development," Idaho National Laboratory, INL/EXT-10-19149, 2011.

[4] J. Daw, J. Rempe and S. Wilkins, "Ultrasonic Thermometry for In-Pile Temperature Detection," in *7th International Topical Meeting on Nuclear Plant Instrumentation, Control, and Human Machine Interface Technologies*, Las Vegas NV, 2010.

[5] X. Sun, B. Lin, J. Bao, V. Giurgiutiu, T. Knight, P. Lam and L. Yu, "Developing a structural health monitoring system for nuclear dry cask storage container," in *SPIE Smart Structures and Materials + Nondestructive Evaluation and Health Monitoring*, San Diago CA, 2015.

[6] C. Lin, H. Chen, M. Tewolde, G. Fu, D. Liu, T. Zhang, H. Tao, C. Nie, W. Zheng, F. Liu, L. Zuo, D. Hwang and J. Longtin, "Thermoelectrically Powered Sensing for Small Modular Reactors," in *ASME Heat Transfer Summer Conference*, Minneapolis MN, 2013.

[7] K. Holbert, S. McCready, A. Heger and T. Harlow, "Performance of Commercial Off-the-Shelf Sensors in a Pulsed Reactor Environment," in *23rd Hardened Electronics and Radiation Technology conference*, Tampa FL, 2005.

[8] N. Anheiser and e. al, "Technical Readiness and Gaps Analysis of Commercial Optical Materials and Measurement Systems for Advanced Small Modular Reactors," Pacific Northwest National Laboratory, PNNL-22622, 2013.

[9] K. Korsah and e. al, "Assessment of Sensor Technologies for Advanced Reactors," Oak Ridge National Laboratory, TM-2016/337 R1, 2016.

[10] D. Ng and G. Fralick, "Temperature Measurement of Beryllia Ceramic Surface in the Presence of Reflected Extraneous Radiation Using a Multiwavelength Pyrometer," NASA TM 2001-210891, 2001.

[11] H. Hashemian and J. Jiang, "Nuclear plant temperature instrumentation," *Nuclear Engineering and Design,* vol. 239, pp. 3132-3141, 2009.

[12] T. Zhu, T. Ke, Y. Rao and K. Chiang, "Fabry-Perot optical fiber tip sensor for high temperature measurement," *Optics Communications,* vol. 283, pp. 3683-3685, 2010.

[13] A. Gusarov and S. Hoeffgen, "Radiation effects on fiber gratings," *IEEE Transactions on Nuclear Science,* vol. 60, pp. 2037-2053, 2013.

[14] A. Morana, S. Girard, E. Marin, J. Perisse, J. Genot, J. Kuhnhenn, J. Grelin, L. Hutter, G. Melin, L. Lablonde, T. Robin, B. Cadier, J. Mace, A. Boukenter and Y. Ouerdane, "Radiation-Hardened Fiber Bragg Grating Based Sensors for Harsh Environments," *IEEE Transactions on Nuclear Science,* vol. 64, pp. 68-73, 2017.

[15] J. Kuhnhenn, U. Weinand, A. Morana, S. Girard, E. Marin, J. Perisse, J. Genot, J. Grelin, L. Hutter, G. Melin, L. Lablonde, T. Robin, B. Cadier, J. Mace, A. Boukenter and Y. Ouerdane, "Gamma Radiation Tests of Radiation Hardened Fiber Bragg Grating-Based Sensors for Radiation Environments," *IEEE Transactions on Nuclear Science,* vol. 64, pp. 2307-2311, 2017.

[16] G. Cheymol, A. Gusarov, S. Gaillot, C. Destouches and N. Caron, "Dimensional Measurements Under High Radiation With Optical Fibre Sensors Based on White Light Interferometry - Report on Irradiation Tests," *IEEE Transactions on Nuclear Science,* vol. 61, pp. 2075-2081, 2014.

[17] A. Sang, M. Froggatt, D. Gifford and B. Dickerson, "One centimeter spatial resolution temperature measurements from 25 to 850 C using Rayleigh scatter in gold coated fiber," in *Conference on Lasers and Electro-Optics*, Baltimore MD, 2007.

[18] C. Petrie, D. Hawn, W. Windl and T. Blue, "Reactor radiation-induced attenuation in fused silica fibers heated up to 1000 C," *Journal of Non-Crystalline Solids,* vol. 409, pp. 88-94, 2015.

[19] D. Sporea and A. Sporea, "Radiation effects in sapphire optical fibers," *Physica Status Solidi C,* vol. 4, pp. 1356-1359, 2007.

[20] M. Busch, W. Ecke, I. Latka, D. Fischer, R. Willsch and H. Bartelt, "Inscription and characterization of Bragg gratings in single-crystal sapphire optical fibres for high-temperature sensor applications," *Measurement Science and Technology,* vol. 20, pp. 115301 - 1-6, 2009.

[21] C. Jewart, Q. Wang, J. Canning, D. Grobnic, S. Mihailov and K. Chen, "Ultrafast femtosecond-laser-induced fiber Bragg gratings in air-hole microstructured fibers for high-temperature pressure sensing," *Optics Letters,* vol. 35, pp. 1443-1445, 2010.

[22] K. Woloshun, M. Merrigan and E. Critchley, "High Temperature Heat Pipe Experiments in Low Earth Orbit," in *National Heat Transfer Conference*, Atlanta GA, 1993.

[23] P. Meisel, S. Schone, W. Lippman, M. Raddatz, A. Hurtado and U. Gampe, "Material Selection, Manufacturing and Performance Test of Ceramic High-Temperature Heat Pipes Using Liquid Metals as Working Fluids," *Advanced Engineering Materials,* vol. 16, pp. 1243-1251, 2014.

[24] M. Le Berre, G. Pandraud and P. Morfouli, "The performance of micro heat pipes measured by integrated sensors," *Journal of Micromechanics and Microengineering,* vol. 16, pp. 1047-1050, 2006.

[25] B. Bercu, L. Montes and P. Morfouli, "SOI built-in heat spreader with temperature and pressure integrated sensors for cooling optimization and in situ monitoring," *Materials Science and Engineering B,* vol. 176, pp. 305-310, 2011.

[26] Idaho National Laboratory, "In-Pile Instrumentation (I2) 2018 Report," July 2019.

[27] Idaho National Laboratory, "Out-of-Pile Performance of High Temperature Irradiation Resistant and Cladding Thermocouples," August 2019.

[28] Idahoe National Laboratory, "Out-of-Pile Testing of Radaiton Hard Optical Fibers," July 2019.

[29] Idaho National Laboratory, "Performance of the supplemental instrumentation in the ATR AGR 5/6/7 irradiation," Advanced Sensors and Instrumentation Annual Webinar, November 2018.

[30] Idaho National Laboratory, "In-Pile Characterization Testing of Gadolinium Self-Powered Neutron Detectors," August 2019.

[31] M. Prowant, G. Dib, H. Qiao, M. Good, M. Larche, S. Sexton and P. Ramuhalli, "Preliminary Design of High Temperature Ultrasonic Transducers for Liquid Sodium Environments," in *Review of Progress in Quantitative Nondestructive Examination, 1949,*, 2017.

[32] B. D. a. P. W. Bowler AI, "An Investigation into the Feasibility of Internal Strain Measurement in Solids by Correlation of Ultrasonic Images," *Proceedings of the Royal Society A: Mathematical, Physical and Engineering Sciences,* vol. 467, no. 2132, pp. 2247-2270, 2011.

[33] A. e. a. Casella, "Complete Initial Ultrasonic Sensor Prototype Design and Preliminary Evaluation," Pacific Northwest National Laboratory, June 2019.

[34] P. Ramuhalli, J. Daw, A. Casella, R. Jacob, M. Good and R. Montgomery, "Ultrasonic Sensors for Fuel Dimensional Monitoring During Transient Irradiation," in *ANS NPIC-HMIT 2019*, Orlando, Florida, 2019.

[35] I. A. Rastegaev, D. L. Merson, A. V. Danyuk, M. A. Afanas’ev and A. K. Khrustalev, "Universal Waveguide for the Acoustic-Emission Evaluation of High-Temperature Industrial Objects," *Russian Journal of Nondestructive Testing,* vol. 54, no. 3, pp. 164-173, 2018.

[36] P. Ramuhalli, G. Dib, M. Prowant, H. Qiao, E. Hirt, C. Lissenden and B. Tittmann, "Assessment of Nondestructive Measurement Sensitivity for Selected Measurement Techniques," Advanced Reactor Technology Milestone: M3AT-17PN2301034, 2017.

[37] W. Xu, C. Lai and X. Sun, "Identify structural flaw location and type with an inverse algorithm of resonance inspection," *Journal of Vibration and Control,* vol. 21, no. 13, pp. 2685-2696, 2015.

[38] P. M. e. al., "Design of Megawatt Power Level Heat Pipe Reactors," Los Alamos National Laboratory, 2015.

[39] M. Sutton, J. Orteu and H. Schreier, Image Correlation for Shape, Motion and Deformation Measurements: Basic Concepts, Theory and Applications, Springer, 2009.

[40] S. Baker and I. Matthew, "Equivalence and Efficiency of Image Alignment Algorithms," in *IEEE Conference on Computer Vision and Pattern Recognition*, 2001.

[41] P. Luo, Y. Chao, M. Sutton and W. Peter, "Accurate measurement of three-dimensional deformations in deformable and rigid bodies using computer vision," *Experimental Mechanics,* vol. 33, pp. 123-132, 1993.

[42] B. Pan, D. Wu, Z. Wang and Y. Xia, "High-temperature digital image correlation method for full-field deformation measurement at 1200 C," *Measurement Science and Technology,* vol. 22, pp. 015701- 1-11, 2011.

[43] R. Berke and J. Lambros, "Ultraviolet digital image correlation (UV-DIC) for high temperature applications," *Review of Scientific Instruments,* vol. 85, pp. 045121- 1-9, 2014.

[44] B. Grant, H. Stone, P. Withers and M. Preuss, "High-temperature strain field measurement using digital image correlation," *Journal of Strain Analysis for Engineering Design,* vol. 44, pp. 263-271, 2009.

[45] X. Guo, J. Liang, Z. Tang, B. Cao and M. Yu, "High-temperature digital image correlation method for full-field deformation measurement captured with filters at 2600 C using spraying to form speckle patterns," *Optical Engineering,* vol. 53, pp. 063101- 1-13, 2014.

[46] Photron, "Meet Crysta," [Online]. Available: https://photron.com/crysta-polarization-high-speed-camera/. [Accessed 5 July 2019].

[47] J. Czarske, E. Scharf and R. Kuschmierz, "Fast 3D Imaging With Lensless Holographic Endoscopy Employing Coherent Fiber Bundles," in *Frontiers in Optics/Laser Science*, Washington DC, 2019.

[48] B. Deng, X. Wang, C. Wu, Y. Qin and H. Wang, "THz-SAR Vibrating Target Imaging via the Bayesian Method," *International Journal of Antennas and Propagation,* pp. 3706925 - 1-10, 2017.

[49] J. Fienup, "Phase Retrieval for Image Reconstruction," *Imaging and Applied Optics,* pp. CM1A.1 - 1-2, 2019.

[50] L. Zhong, P. Konda, M. Harfouche and R. Horstmeyer, "Depth tracking using a multi-aperture microscope," *Imaging and Applied Optics,* pp. CTh4A.2 - 1-2, 2019.

[51] P. Rangarajan, I. Sinharoy, P. Milojkovic and M. Christensen, "Active computational imaging for circumventing resolution limits at macroscopic scales," *Applied Optics,* vol. 56, pp. D84-D107, 2017.

[52] F. Schiffers, F. Willomitzer, P. Ruiz, A. Katsaggelos and O. Cossairt, "Speckle based Extended Depth-of-field for Macroscopic Imaging: First Results," *Imaging and Applied Optics,* pp. CTh4A.6 - 1-2, 2019.

[53] C. Callenberg, A. Lyons, D. den Brok, R. Henderson, M. Hullin and D. Faccio, "EMCCD-SPAD Camera data fusion for high spatial resolution time-of-flight imaging," *Imaging and Applied Optics,* pp. CTh2A.3 - 1-2, 2019.

[54] A. Pawlikowska, A. Halimi, R. Lamb and G. Buller, "Single-photon three-dimensional imaging at up to 10 kilometers range," *Optics Express,* vol. 25, pp. 286022 - 1-13, 2017.

[55] Z. Li, X. Huang, Y. Cao, B. Wang, Y. Li, J. Zhang, Q. Zhang, C. Peng, F. Xu and J. Pan, "Photon-efficient 3D imaging up to 21.6 km," *Imaging and Applied Optics,* pp. CTh2A.4 - 1-2, 2019.

[56] T. Pittman, Y. Shih, V. Strekalov and A. Sergienko, "Optical imaging by means of two-photon quantum entanglement," *Physical Review A,* vol. 52, pp. R3429 - 1-4, 1995.

[57] A. Gatti, M. Bache, D. Magatti, E. Brambilla, F. Ferri and L. Lugiato, "Coherent imaging with pseudo-thermal incoherent light," *Journal of Modern Optics,* vol. 53, pp. 739-760, 2006.

[58] J. Shapiro, "Computational Ghost Imaging," *Physical Review A,* vol. 78, pp. 061802 - 1-4, 2008.

[59] Y. Bromberg, O. Katz and Y. Silberberg, "Ghost imaging with a single detector," *Physical Review A,* vol. 79, pp. 053840 - 1-4, 2009.

[60] M. Okaji and H. Imai, "A high-temperature dilatometer using optical heterodyne interferometry," *Journal of Physics E: Scientific Instruments,* vol. 20, pp. 887-891, 1987.

[61] T. Aurora, S. Day, V. King and D. Pederson, "High-temperature laser interferometer for thermal expansion and optical-length measurements," *Review of Scientific Instruments,* vol. 55, pp. 149-152, 1984.

[62] O. Lokberg, J. Malmo and G. Slettemoen, "Interferometric measurements of high temperature objects by electronic speckle pattern interferometry," *Applied Optics,* vol. 24, pp. 3167-3172, 1985.

[63] K. Stetson, "The Use of Heterodyne Speckle Photogrammetry to Measure High-Temperature Strain Distributions," in *Holographic Data Nondestructive Testing*, Dubrovnik, Croatia, 1982.

[64] D. Evenson, R. Aprahamian and K. Overoye, "Pulsed Differential Holographic Measurements of Vibration Modes," NASA CR-2028, 1972.

[65] D. Post, B. Han and P. Ifju, High Sensitivity Moire: Experimental Analysis for Mechanics and Materials, Springer, 1994.

[66] C. Forno, "High-temperature-resistant gratings for moire interferometry," in *International Conference on Interferometry*, Warsaw, 1994.

[67] T. Hyde, H. Xie, W. Sun, F. Dai and D. Zou, "High Temperature Gratings for the Moire and Moire Interferometry Methods and their Application of Deformation Measurement - A Review," *Strain,* vol. 37, pp. 59-66, 2001.

[68] G. Cloud and C. Bayer, "Moire to 1370 C," *Experimental Techniques,* vol. 12, no. 4, pp. 24-27, 1988.

[69] B. Kang, X. Liu, C. Cisloiu and K. Chang, "High temperature moire interferometry investigation of creep crack growth of inconel 783-environment and beta-phase effects," *Materials Science and Engineering A,* vol. 347, pp. 205-213, 2003.

[70] E. Candes and M. Wakin, "An Introduction to Compressive Sampling," *IEEE Signal Processing Magazine,* pp. 21-30, March 2008.

[71] M. Rani, S. Dhok and R. Deshmukh, "A Systematic Review of Compressive Sensing: Concepts, Implementations and Applications," *IEEE Access,* vol. 6, pp. 4875-4894, 2018.

[72] Z. Zou, Y. Bao, H. Li, B. Spencer Jr and J. Ou, "Embedding Compressive Sensing-Based Data Loss Recovery Algorithm Into Wireless Smart Sensors for Structural Health Monitoring," *IEEE Sensors Journal,* vol. 15, pp. 797-808, 2015.

[73] B. Brunton, S. Brunton, J. Proctor and J. Kutz, "Sparse sensor placement optimization for classification," *SIAM Journal of Applied Mathematics,* vol. 76, pp. 2099-2122, 2016.

[74] S. Mekhail, N. Abudukeyoumu, J. Ward, G. Arbuthnott and S. Chormaic, "Fiber-bundle-basis sparse reconstruction for high resolution wide-field microendoscopy," *Biomedical Optics Express,* vol. 9, pp. 1843-1851, 2018.

[75] H. Chen, M. Asif, A. Sankaranarayanan and A. Veeraraghavan, "FPA-CS: Focal Plane Array-based Compressive Imaging in Short-wave Infrared," in *Computer Vision and Pattern Recognition*, Boston, 2015.

[76] Q. Zhou, J. Ke and E. Lam, "Dual-waveband Temporal Compressive Imaging," *Imaging and Applied Optics,* pp. CTu2A.8 - 1-2, 2019.

[77] S. George, N. Augustine and D. Pattathil, "Audio security through compressive sampling and cellular auotmata," *Multimedia Tools and Applications,* vol. 74, pp. 10393-10417, 2015.

[78] Y. Arjoune, N. Kaabouch, H. Ghazi and A. Tamtaoui, "A performance comparison of measurement matrices in compressive sensing," *International Journal of Communication Systems,* vol. 31, pp. e3576 - 1-18, 2018.

[79] M. O'Toole, D. Lindell and G. Wetzstein, "Confocal non-line-of-sight imaging based on the light-cone transform," *Nature,* vol. 555, pp. 338-341, 2018.

[80] S. Xin, S. Nousias, K. Kutulakos, A. Sankaranarayanan, S. Narasimhan and I. Gkioulekas, "A Theory of Fermat Paths for Non-Line-of-Sight Shape Reconstruction," in *IEEE Computer Vision and Pattern Recognition*, Long Beach CA, 2019.

[81] G. Musarra, A. Lyons, E. Conca, Y. Altmann, F. Villa, F. Zappa, M. Padgett and D. Faccio, "Non-Line-of-Sight Three-Dimensional Imaging with a Single-Pixel Camera," *Physical Review Applied,* vol. 12, pp. 011002 - 1-6, 2019.

[82] D. Faccio and A. Velten, "A trillion frames per second: the techniques and applications of light-in-flight photography," *Reports on Progress in Physics,* vol. 81, pp. 105901 - 1-22, 2018.

[83] D. Lindell, G. Wetzstein and V. Koltun, "Acoustic Non-Line-of-Sight Imaging," in *IEEE Computer Vision and Pattern Recognition*, Long Beach CA, 2019.

[84] T. Maeda, Y. Wang, R. Raskar and A. Kadambi, "Thermal Non-Line-of-Sight Imaging," in *IEEE International Conference on Computational Photography*, Tokyo, 2019.

[85] M. Batarseh, S. Sukhov, Z. Shen, H. Gemar, R. Rezvani and A. Dogariu, "Passive sensing around the corner using spatial coherence," *Nature Communications,* vol. 9, pp. 3629 - 1-6, 2018.

[86] A. Kadambi, H. Zhao, B. Shi and R. R, "Occluded Imaging with Time-of-Flight Sensors," *ACM Transactions on Graphics,* vol. 35, pp. 15 - 1-12, 2016.

[87] A. Velten, T. Willwacher, O. Gupta, A. Veeraraghavan, M. Bawendi and R. Raskar, "Recovering three-dimensional shape around a corner using ultrafast time-of-flight imaging," *Nature Communications,* vol. 3, pp. 745 - 1-8, 2012.

[88] J. Klein, C. Peters, J. Martin, M. Laurenzis and M. Hullin, "Tracking objects outside of line of sight using 2D intensity images," *Scientific Reports,* vol. 6, pp. 32491 - 1-9, 2016.

[89] F. Willomitzer, F. Li, M. Balaji, P. Rangarajan and O. Cossairt, "High Resolution Non-Line-of-Sight Imaging with Superheterodyne Remote Digital Holography," *Imaging and Applied Optics,* pp. CM2A.2 - 1-2, 2019.

[90] X. Liu, I. Guillen, M. La Manna, J. Nam, S. Rez, T. Le, A. Jarabo, D. Gutierrez and A. Velten, "Non-line-of-sight imaging using phasor-field virtual wave optics," *Nature,* 5 August 2019.

[91] I. Dokmanic, R. Parhizkar, A. Walther, Y. Lu and M. Vetterli, "Acoustic echoes reveal room shape," *Proceedings of the National Academy of Sciences,* 2013.

[92] D. Lin, L. J and C. Hashemi, "Non-Line-of-Sight Imaging using Plenoptic Information," *Imaging and Applied Optics,* pp. CM2A.5 - 1-2, 2019.

[93] G. Satat, B. Heshmat, D. Raviv and R. Raskar, "All Photons Imaging Through Volumetric Scattering," *Scientific Reports,* vol. 6, pp. 33946 - 1-8, 2016.

[94] A. Boccolini, G. Tonolini, J. Leach, R. Henderson and D. Faccio, "Imaging inside highly diffuse media with a space and time-resolving single-photon sensor," *Imaging and Applied Optics,* pp. iTu3E.2 - 1-2, 2017.

[95] G. Kuo, N. Antipa, R. Ng and L. Waller, "DiffuserCam: Diffuser-Based Lensless Cameras," *Imaging and Applied Optics,* pp. CTu3B.2 - 1-3, 2017.

[96] N. Antipa, G. Kuo, R. Ng and L. Waller, "3D DiffuserCam: Single-Shot Compressive Lensless Imaging," *Imaging and Applied Optics,* pp. CM2B.2 - 1-3, 2017.

[97] T. Nakamura, K. Kagawa, S. Torashima and M. Yamaguchi, "Super Field-of-View Lensless Camera by Coded Image Sensors," *Sensors,* vol. 19, pp. 1329 - 1-13, 2019.

[98] O. Katz, P. Heidmann, M. Fink and S. Gigan, "Non-invasive single-shot imaging through scattering layers and around corners via speckle correlations," *Nature Photonics,* vol. 8, pp. 784-790, 2014.

[99] X. Sun, Y. Wang and J. Fleischer, "Seeing through a scattering medium using a folded-wave coherence interferometer," *Imaging and Applied Optics,* pp. CTu4A.2 - 1-2, 2019.

[100] X. Li, J. Greenberg and M. Gehm, "Single-shot Multispectral Color Imaging Through Scattering Media," *Imaging and Applied Optics,* pp. CTu4A.3 - 1-2, 2019.

[101] R. Stolt and A. Weglein, Seismic Imaging and Inversion: Application of Linear Inverse Theory, Cambridge, 2012.

[102] E. Robien, Seismic Imaging: A Review of the Techniques, their Principles, Merits and Limitations, EAGE, 2010.

[103] R. Burridge, "The Gelfand-Levitan, the Marchenko, and the Gopinath-Sondhi Integral Equations of Inverse Scattering Theory, Regareded in the Context of Inverse Impulse Response Problems," *Wave Motion,* vol. 2, pp. 305-323, 1980.

[104] D. Ge, "An iterative technique in one-dimensional profile inversion," *Inverse Problems,* vol. 3, pp. 399-406, 1987.

[105] F. Broggini and R. Snieder, "Connection of scattering principles: a visual and mathermatical tour," *European Journal of Physics,* vol. 33, pp. 593-613, 2012.

[106] K. Wapenaar, J. Thorbecke, J. van der Neut, F. Broggini, E. Slob and R. Snieder, "Marchenko Imaging," *Geophysics,* vol. 79, pp. WA39-WA57, 2014.

[107] S. Singh, "An Inverse Scattering Approach to Imaging Using Marchenko Equations in the Presence of a Free Surface," PhD thesis, Colorado School of Mines, 2016.

[108] M. Matias, R. Pestana and J. van der Neut, "Marchenko imaging by unidimensional deconvolution," *Geophysical Prospecting,* vol. 66, pp. 1653-1666, 2018.

[109] X. Maldague, Nondestructive Evaluation of Materials by Infrared Thermography, Springer-Verlag, 1993.

[110] P. Reynolds, "A review of multicolour pyrometry for temperatures below 1500 C," *British Journal of Applied Physics,* vol. 15, pp. 579-589, 1964.

[111] D. DeWitt, "Inferring temperature from optical radiation measurements," *Optical Engineering,* vol. 25, pp. 596-601, 1986.

[112] F. Ciampa, P. Mahmoodi, F. Pinto and M. Meo, "Recent Advances in Active Infrared Thermography for Non-Destructive Testing of Aerospace Components," *Sensors,* vol. 18, pp. 609 - 1-37, 2018.

[113] S. Holland, "Thermographic signal reconstruction for vibrothermography," *Infrared Physics & Technology,* vol. 54, pp. 503-511, 2011.

[114] H. Banks, B. Boudreaux, A. Criner, K. Foster, C. Uttal, T. Vogel and W. Winfree, "Thermal-based damage detection in porous materials," *Inverse Problems in Science and Engineering,* vol. 18, pp. 835-851, 2010.

[115] H. Kawakami, "Reconstruction algorithm for unknown cavities via Feynman-Kac type formula," *Computer Optimization and Applications,* vol. 61, pp. 101-133, 2015.

[116] M. Fink, "Time Reversed Acoustics," *Physics Today,* vol. 50, no. 3, pp. 34-40, March 1997.

[117] M. Willardson, B. Anderson, S. Young, M. Dension and B. Patchett, "Time reversal focusing of high amplitude sound in a reverberation chamber," *Journal of the Acoustical Society of America,* vol. 143, pp. 696-705, 2018.

[118] P. Blomgren, G. Papanicolaou and H. Zhao, "Super-resolution in time-reversal acoustics," *Journal of the Acoustical Society of America,* vol. 111, pp. 230-248, 2002.

[119] A. Pradzka, S. Feat and P. Petitjeans, "Time Reversal of Water Waves," *Physical Review Letters,* vol. 109, pp. 064501 - 1-5, 2012.

[120] J. de Rosny, G. Lerosey, A. Tourin and M. Fink, "Time Reversal of Electromagentic Waves," in *Modeling and Computations in Electromagnetics*, H. Ammari, Ed., Springer, 2008, pp. 187-202.

[121] M. Wimmer and U. Peschel, "Observation of Time Reversed Light Propagation by an Exchange of Eigenstates," *Scientific Reports,* vol. 8, pp. 2125 - 1-7, 2018.

[122] P. MS, G. Dib, H. Qiao, M. Good, M. Larche, S. Sexton and P. Ramuhalli., "Preliminary design of high temperature ultrasonic transducers for liquid sodium environments," in *AIP Conference Proceedings 1949, 100006 (2018)*, 2017.